Identification and inhibition of the ICE/CED-3 protease necessary for mammalian apoptosis

Donald W. Nicholson*, Ambereen Ali*, Nancy A. Thornberry†, John P. Vaillancourt*, Connie K. Ding‡, Michel Gallant§, Yves Gareau§, Patrick R. Griffin‡, Marc Labelle§, Yuri A. Lazebnik‖, Neil A. Munday*, Sayyaparaju M. Raju‡, Mark E. Smulson¶, Ting-Ting Yamin‡, Violeta L. Yu* & Douglas K. Miller‡

Departments of * Biochemistry and Molecular Biology, and § Medicinal Chemistry, Merck Frosst Centre for Therapeutic Research, PO Box 1005, Pointe Claire-Dorval, Quebec, H9R 4P8 Canada
Departments of † Biochemistry and ‡ Inflammation Research, Merck Research Laboratories, PO Box 2000, Rahway, New Jersey 07065, USA
‖ Cold Spring Harbor Laboratory, PO Box 100, Cold Spring Harbor, New York 11724, USA
¶ Department of Biochemistry and Molecular Biology, Georgetown University School of Medicine, 3900 Reservoir Road NW, Washington DC, USA

The protease responsible for the cleavage of poly(ADP-ribose) polymerase and necessary for apoptosis has been purified and characterized. This enzyme, named apopain, is composed of two subunits of relative molecular mass (M_r) 17K and 12K that are derived from a common proenzyme identified as CPP32. This proenzyme is related to interleukin-1β-converting enzyme (ICE) and CED-3, the product of a gene required for programmed cell death in *Caenorhabditis elegans*. A potent peptide aldehyde inhibitor has been developed and shown to prevent apoptotic events *in vitro*, suggesting that apopain/CPP32 is important for the initiation of apoptotic cell death.

Apoptosis constitutes a systematic means of cell suicide within an organism during normal morphogenesis, tissue remodelling and in response to pathogenic infections or other irreparable cell damage. Inappropriate apoptosis may underlie the aetiology of human diseases such as Alzheimer's, Parkinson's and Huntington's diseases, immune deficiency and autoimmune disorders, ischaemic cardiovascular and neurological injury, alopecia, leukaemias, lymphomas and other cancers, which therefore makes the control of apoptosis an important potential target for therapeutic intervention[1–4].

Several of the biochemical events that contribute to apoptotic cell death have recently been elucidated. Genetic evidence in nematodes, for example, has identified both positive and negative regulators of apoptosis[5]. The key pro-apoptotic gene, *ced-3*, encodes a putative cysteine protease that is related to mammalian interleukin-1β-converting enzyme (ICE)[6], the first identified member of a new family of cysteine proteases with the distinguishing feature of a near-absolute specificity for aspartic acid in the S_1 subsite[7,8]. Deletion or mutation of the *ced-3* gene completely prevented the apoptotic death of all cells that were otherwise destined to die, and both CED-3 and ICE induced apoptosis when transfected into a variety of host cells[6,9,10]. Furthermore, the pro-apoptotic effects of CED-3 could be prevented by the nematode cell-death suppressor gene *ced-9*, and to some degree by its mammalian counterpart, the proto-oncogene *bcl-2*. The fate of eukaryotic cells may therefore reside in the balance between the opposing pro-apoptotic effects of an ICE/CED-3-like protease and an upstream regulatory mechanism involving Bcl-2 and/or its homologues.

One of the potential substrates for an ICE/CED-3-like protease during apoptosis is poly(ADP-ribose) polymerase (PARP), an enzyme that appears to be involved in DNA repair, genome surveillance and integrity[11–17], predominantly in response to environmental stress[18]. PARP is proteolytically cleaved at the onset of apoptosis by a hitherto-unidentified protease with properties that resemble those of ICE[19,20]. The cleavage site within PARP (DEVD 216–G 217) resembles one of the two sites in proIL-1β (FEAD 27–G 28) that are recognized and cleaved by ICE. Proteolytic cleavage of PARP at this site results in the separation of the two zinc-finger DNA-binding motifs in the amino terminus of PARP from the automodification and poly(ADP-ribos)ylating catalytic domains located in the carboxy terminus of the polypeptide. This cleavage precludes the catalytic domain of PARP from being recruited to sites of DNA damage, and presumably disables PARP from coordinating subsequent repair and genome maintenance events. Furthermore, the Ca^{2+}/Mg^{2+}-dependent endonuclease implicated in the internucleosomal DNA cleavage that is a hallmark of apoptosis is negatively regulated by poly(ADP-ribos)ylation[21–23]. Loss of normal PARP function may therefore render this nuclease highly activated in dying cells.

The five known members of the ICE/CED-3 family of cysteine proteases which are of human origin are ICE, ICE_{rel}-II, ICE_{rel}-III, Nedd-2/ICH-1 and CPP-32 (refs 24–27). Each is capable of initiating an apoptotic response when transfected into host cells; however, it is possible that overexpression of any protease may cause nonspecific induction of cell death. Cytoplasmic expression of other proteases, such as trypsin, chymotrypsin, proteinase K or granzyme B, for example, have also been shown to induce apoptosis[28,29].

Here we demonstrate that an active form of CPP-32, for which the name apopain is proposed, is the enzyme responsible for the specific proteolytic breakdown of PARP that occurs at the onset of apoptosis. Furthermore, we show that inhibition of CPP-32/apopain-mediated PARP cleavage attenuates apoptosis *in vitro*, demonstrating the importance of this protease in the apoptosis of mammalian cells.

PARP cleavage activity

An early event that occurs concomitantly with the onset of apoptosis is the proteolytic breakdown of PARP by an unidentified protease with properties resembling those of ICE (prICE)[20]. The resulting cleavage (between Asp 216 and Gly 217) separates the N-terminal DNA-nick sensor of PARP from its C-terminal catalytic domain (Fig. 1*a*). To measure this proteolytic activity, [^{35}S]PARP was generated as a substrate by *in vitro* transcription/translation of a full-length human PARP complementary DNA clone and was then combined with various cell extracts (Fig. 1*b*). A human osteosarcoma cell line with a propensity for spontaneous apoptotic death contained substantial PARP cleavage activity that was markedly higher in extracts from apoptotic cells versus non-apoptotic cells (lanes 2 and 3, respectively). Osteosarcoma cells are a good model system for studying the events that occur during apoptosis. Upon reaching confluence in culture they undergo the morphological and biochemical changes characteristic of apoptotic death, including cell shrinkage, membrane blebbing, chromatin condensation and fragmentation (not shown), as well as internucleosomal DNA cleavage (Fig. 1*c*). Coincident with the progressive apoptosis that occurred in postconfluent osteosarcoma cell cultures, the PARP cleavage activity measured in cell extracts was elevated more than tenfold (Fig. 1*d*). There was no detectable ICE in these extracts, as judged by immunoblotting, reverse-transcriptase polymerase chain reaction (RT–PCR) (not shown), and by the absence of proIL-1β processing, indicating that ICE is not necessary for apoptosis or for PARP cleavage. The lack of a major role for ICE in apoptosis was confirmed in ICE-deficient mice where apoptosis largely occurred normally[30,31], although a potential role for ICE in Fas-mediated thymocyte apoptosis has been suggested[32,33].

PARP cleavage activity was also measurable in cytoplasmic extracts of THP-1 cells, the human monocytic leukaemia cell line from which ICE was originally purified, particularly after pre-incubation of the extracts at 37 °C (Fig. 1*b*, lanes 4 and 5). This suggests that the PARP cleavage enzyme requires activation of a latent form, as has been described for ICE in this cell line[34]. PARP cleavage in apoptotic osteosarcoma cell extracts and activated THP-1 cell extracts was comparable to that in apoptotic chicken S/M extracts (lane 6; S/M extracts were prepared from chicken hepatoma cells committed to apoptosis by sequential synchronization in the S phase and mitosis), where this proteolytic activity was originally identified[20].

Inhibitors of PARP cleavage

The proteolytic cleavage of PARP in cytosolic extracts from apoptotic osteosarcoma cells was abolished by the cysteine-alkylating reagents *N*-ethylmaleimide and iodoacetamide, but not by E-64 (also a cysteine-protease inhibitor) or by inhibitors of serine-, aspartate- or metallo-proteases (Fig. 2*a*). This inhibitor profile is consistent with the PARP cleavage enzyme being a member of the emerging ICE-like family of cysteine proteases. To develop more potent and specific PARP cleavage inhibitors, the sequences proximal to the scissile bond were used as a template for inhibitor design. Appropriate peptide aldehydes can be

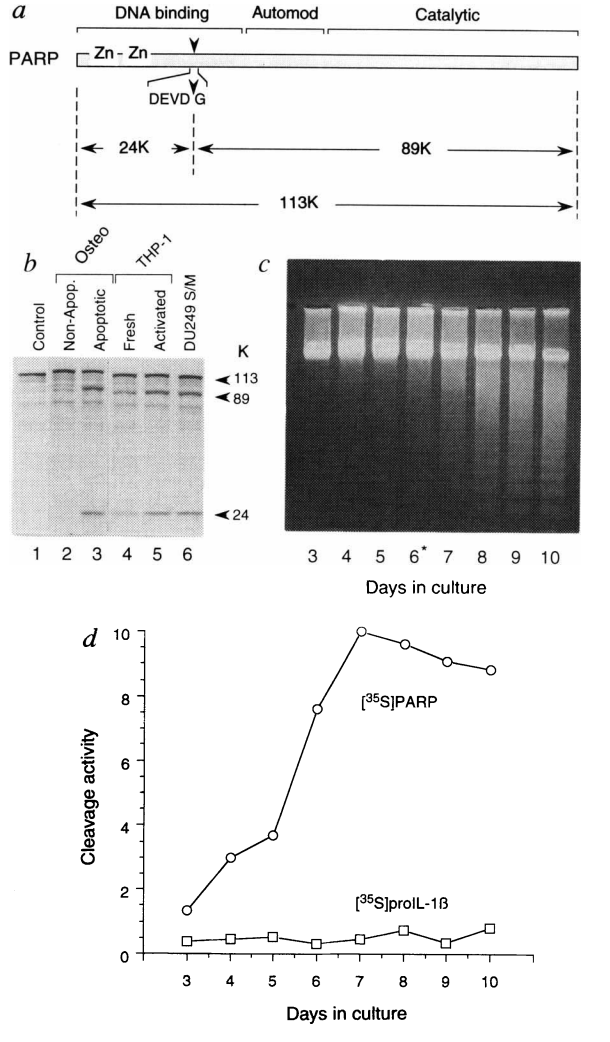

FIG. 1 PARP cleavage activity in spontaneously apoptotic osteosarcoma cells. *a*, Structure of PARP[42] and fragments resulting from proteolytic cleavage[20]. *b*, *In vitro* cleavage of PARP by cell extracts. [^{35}S]PARP was generated by *in vitro* transcription/translation then combined with cytosolic extracts from pre-confluent, non-apoptotic osteosarcoma cells (4.5 μg, lane 2), postconfluent, apoptotic osteosarcoma cells (4.5 μg, lane 3), freshly isolated THP-1 cells (30 μg, lane 4), THP-1 cell extracts activated by preincubation for 60 min at 37 °C (30 μg, lane 5), or apoptotic chicken S/M extracts (0.6 μg, lane 6). *c*, Internucleosomal DNA cleavage in progressively apoptotic osteosarcoma cells. Osteosarcoma cells were maintained in culture for the indicated number of days and then collected. DNA was extracted and resolved on agarose gels. An asterisk indicates the time point (day 6) where confluence was reached. *d*, Elevation of PARP cleavage activity in progressively apoptotic osteosarcoma cells. Cytosol fractions were isolated from cells described in *c* and then assayed for PARP cleavage activity (circles) and proIL-1β cleavage activity (squares).

METHODS. Cytosolic extracts were prepared from cultured human osteosarcoma cells (143.98.2; ATCC CRL 11226) and THP-1 cells (ATCC TIB 202) by homogenizing PBS-washed cell pellets in 10 mM HEPES/KOH (pH 7.4), 2 mM EDTA, 0.1% CHAPS, 5 mM dithiothreitol, 1 mM phenylmethylsulphonylfluoride, 10 μg ml^{-1} pepstatin A, 20 μg ml^{-1} leupeptin, 10 μg ml^{-1} aprotinin (at 1×10^8 cells ml^{-1}) and recovering the post 100,000*g* supernatant after centrifugation. Chicken S/M extracts were prepared from DU249 hepatoma cells[43] that were committed to apoptosis by S-phase aphidicolin arrest followed by M-phase accumulation with nocodazole as described previously[41]. The full-length cDNA clone for PARP (pcD-12)[44] was excised and ligated into the *Xho*I site of pBluescript-II SK+ (Stratagene) then used to drive the synthesis of [^{35}S]methionine-labelled PARP by coupled transcription/translation. [^{35}S]PARP cleavage activity was measured essentially as described previously[7] for ICE-dependent cleavage of [^{35}S]proIL-1β, except the pH was 6.5. Data for *d* are the average of two independent experiments.

potent inhibitors of cysteine proteases, as exemplified by the sensitivity of ICE to the tetrapeptide aldehyde Ac-YVAD-CHO ($K_i = 0.76$ nM). A tetrapeptide aldehyde containing the P_1–P_4 amino-acid sequence of the PARP cleavage site (DEVD 216–G 217) was therefore synthesized and found to be a potent inhibitor of PARP breakdown (Ac-DEVD-CHO; Fig. 2*b* inset). Ac-DEVD-CHO inhibited the PARP cleavage activity in apoptotic osteosarcoma cell extracts with a 50% inhibitory concentration (IC_{50}) of 0.2 nM. In contrast, the corresponding carboxylic acid (Ac-DEVD-COOH) and the tetrapeptide aldehyde containing the proIL-1β recognition sequence for ICE (Ac-YVAD-CHO) had IC_{50} values >10 μM (Fig. 2*a*, *b*). An identical inhibitor profile was found for the PARP cleavage activity in activated THP-1 cell extracts and in apoptotic chicken S/M extracts (not shown). The cowpox-virus serpin CrmA (the product of the cytokine-response-modifier A gene, *crmA*), which is a potent inhibitor of ICE[35] ($K_i < 4$ pM), was a very poor inhibitor of PARP cleavage (Fig. 2*c*). PARP cleavage is therefore mediated by an E-64-insensitive cysteine protease that can be inhibited by low concentrations of the tetrapeptide aldehyde Ac-DEVD-CHO but not by high levels of potent inhibitors of ICE.

Purification of PARP cleavage protease

To identify the enzyme responsible for PARP inactivation in mammalian cells during apoptosis, it was purified to homogeneity from cultured human cells. PARP cleavage activity was highly elevated in osteosarcoma cells as they progressed into apoptosis upon reaching confluence; however, owing to the impracticality of obtaining sufficient quantities of an adherent cell line to purify the protease, THP-1 cells were used. Two lines of evidence suggested that the cysteine protease that cleaved PARP in THP-1 cells was the same as that in apoptotic osteosarcoma cells. First, and most compelling, the kinetic parameters for catalysis, and inhibition by Ac-DEVD-CHO, were found to be virtually identical for the enzyme in extracts from both cell types (see below). Second, RT–PCR indicated that, with the exception of ICE (for which transcripts were detectable in THP-1 cells only), both THP-1 cells and apoptotic osteosarcoma cells contained transcripts for the same compliment of ICE/CED-3-

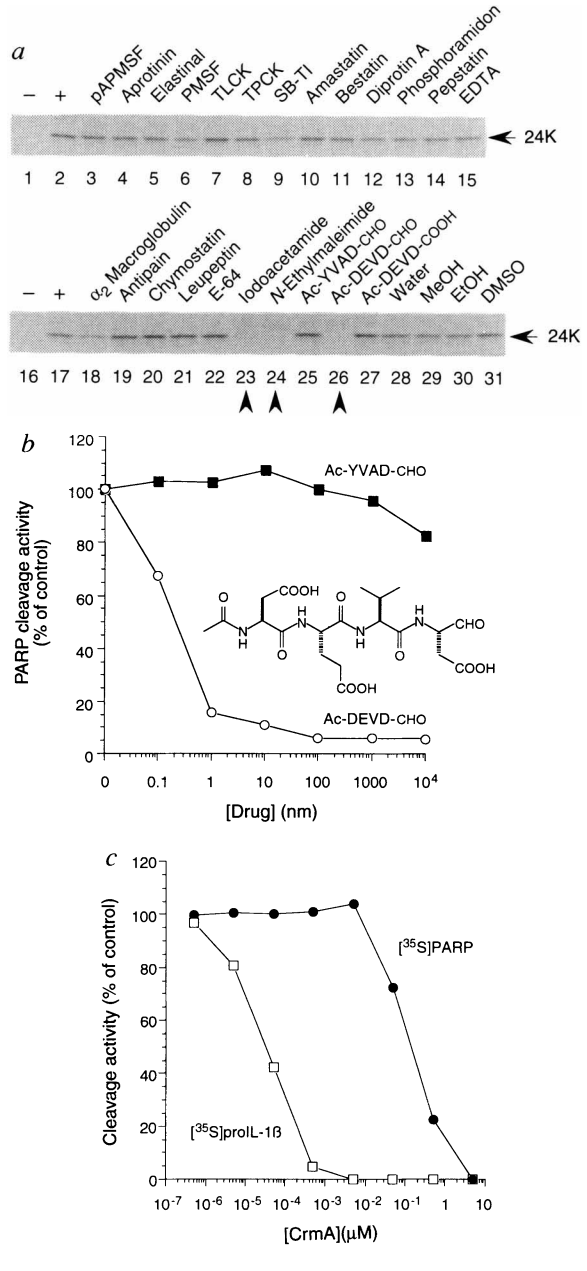

FIG. 2 Inhibition of PARP cleavage in apoptotic osteosarcoma cell extracts. *a*, Inhibition by various protease inhibitors. The cytosol fraction from apoptotic osteosarcoma cells was incubated with [^{35}S]PARP in the presence of various protease inhibitors as indicated. The 24K cleavage product from the resulting fluorogram is shown. *b*, Inhibition by synthetic tetrapeptide aldehydes. The cytosol fraction from apoptotic osteosarcoma cells was incubated with [^{35}S]PARP in the presence of the indicated concentrations of the tetrapeptide aldehyde Ac-DEVD-CHO (open circles, inset) or Ac-YVAD-CHO (filled squares) that were modelled after the P_1–P_4 amino acids of the PARP cleavage site and proIL-1β cleavage site, respectively. *c*, Inhibition by CrmA. [^{35}S]proIL-1β cleavage by purified ICE (open squares) or [^{35}S]PARP cleavage by the purified PARP cleavage enzyme (filled circles) was measured in the presence of the indicated concentrations of CrmA.

METHODS. *a*, [^{35}S]PARP cleavage was measured in incubation mixtures containing 10 μg protein from the cytosol fraction of apoptotic osteosarcoma cells (from 7-day, postconfluent cultures) that were preincubated for 20 min at 37 °C in the presence of 100 μM 4-amidinophenylmethanesulphonylfluoride (pAPMSF), 2 μg ml^{-1} aprotinin, 100 μM elastinal, 1 mM phenylmethylsulphonylfluoride (PMSF), 100 μM L-1-chloro-3-[4-tosylamido]-7-amino-2-heptanone (TLCK), 100 μM L-1-chloro-3-[4-tosylamido]-4-phenyl-2-butanone (TPCK), 1 mg ml^{-1} soybean trypsin inhibitor (SB-TI), 10 μM amastatin, 10 μM bestatin, 50 μM diprotin A, 8.5 μM phosphoramidon, 1 μM pepstatin, 5 mM EDTA, 1 mg ml^{-1} α_2-macroglobulin, 100 μM antipain, 100 μM chymotrypsin, 100 μM leupeptin, 10 μM E-64, 5 mM iodoacetamide, 5 mM *N*-ethylmaleimide, 1 μM Ac-YVAD-CHO, 100 nM Ac-DEVD-CHO, 100 nM Ac-DEVD COOH or vehicle (lanes 28 to 31). b, The tetrapeptide aldehyde Ac-YVAD-CHO was synthesized as described previously[45], and Ac-DEVD-CHO (inset) was synthesized essentially by the same procedure. [^{35}S]PARP cleavage activity was measured in mixtures containing 10 μg protein from the cytosol fraction of apoptotic osteosarcoma cells (from 7-day, postconfluent cultures) that were preincubated for 20 min at 37 °C with the indicated concentrations of Ac-YVAD-CHO (filled squares) or Ac-DEVD-CHO (open circles) before the addition of [^{35}S]PARP. Data are the average of two independent experiments. *c*, Cleavage of [^{35}S]proIL-1β by ICE and cleavage of [^{35}S]PARP by the purified PARP cleavage protease (see Fig. 3) was measured as described for Fig. 1c in the presence of varying concentrations of purified recombinant CrmA.

like enzymes (namely, ICE_{rel}-II, Nedd-2/ICH-1 and CPP-32 but not ICE_{rel}-III) (not shown).

When cytosol fractions from THP-1 cells were resolved by diethylaminoethyl (DEAE) anion-exchange chromatography, the PARP cleavage activity was separated from ICE immunoreactivity and proIL-1β cleavage activity, which coeluted from the column at a lower salt concentration (approximately 80 mM and 100 mM for ICE and PARP cleavage activities, respectively). The fractions containing PARP cleavage activity from several chromatographic runs were pooled and re-chromatographed under identical conditions (Fig. 3*a*). To selectively purify this activity, two biotinylated derivatives of the Ac-DEVD-CHO tetrapeptide aldehyde inhibitor were synthesized as affinity ligands for the PARP cleavage enzyme (Fig. 3*b*). Biotinylated affinity ligands were used because they could be pre-incubated with the enzyme to overcome slow ligand binding (see below), by allowing full equilibrium to occur before collection. Both biotinylated tetrapeptide aldehydes had IC_{50} values for inhibition of the PARP cleavage enzyme that were comparable to that of the non-biotinylated parent compound (0.2 nM; not shown). The DEAE-chromatography fraction at the peak of PARP cleavage activity was incubated with the biotinylated tetrapeptide aldehydes, then collected with streptavidin-agarose. After extensive washing, the purified PARP cleavage enzyme was eluted from the column with 2 mM biotin. SDS–PAGE (polyacrylamide gel electrophoresis) of the resulting samples indicated that the purified PARP cleavage enzyme was composed of two major polypeptides of approximate M_r 17K and 12K (Fig. 3*c*).

Structure of PARP cleavage protease

Electrospray mass spectroscopy analysis of the purified PARP cleavage enzyme indicated that the M_r of the larger polypeptide was 16,617.1 ± 3.1 and the smaller polypeptide was 11,896 ± 1.2 (Fig. 4*a*). N-terminal sequence determination and tryptic maps of the purified enzyme identified it as CPP-32, a member of the ICE/CED-3 family of cysteine protease of unknown function which was recently cloned from Jurkat cells[26]. Cloned CPP-32 was originally identified as two isoforms (CPP-32α and CPP-32β) which differ by a single conservative amino-acid substitution (Asp 190 versus Glu 190 for CPP-32α and CPP-32β, respectively). The N-terminal sequence of the 12K subunit of the purified PARP cleavage enzyme corresponded with that of CPP-32β (Fig. 4*b*), as did the cDNA sequence of human CPP-32 cloned from placenta, lung and kidney (not shown).

Both the mass determination and N-terminal sequence of the two subunits were in agreement, and demonstrated that both polypeptides were derived from the same 32K CPP-32 precursor polypeptide by cleavage between Asp 28–Ser 29 and Asp 175–Ser 176 (Fig. 4*b*). The organization of the CPP-32 proenzyme is similar to that of ICE (Fig. 4*c*). Like ICE, the CPP-32 proenzyme is composed of an N-terminal pro-domain followed by a larger subunit (p17) that contains the putative active site cysteine and histidine residues; this is then followed by the smaller subunit (p12). The major differences between ICE and CPP-32 pro-enzymes are that the pro-domain of CPP-32 is substantially shorter, and there is no linker peptide separating the larger (p17) subunit of CPP-32 from the smaller (p12) subunit. The presence of Asp residues in the P_1 position of both the pro-domain/p17 junction and the p17/p12 junction of CPP-32 suggests that autocatalysis plays an important role in pro-enzyme activation, as has been demonstrated for ICE[7,36,37].

Sequence alignment of all known members of the ICE/CED-3 family of cysteine proteases indicates that CPP-32 is the most closely related of the mammalian enzymes to CED-3, the pro-apoptotic, nematode cell-death-abnormal *ced-3* gene product (Fig. 4*d*). An alignment of the five known human enzymes in this family and CED-3 indicates that there is absolute conservation of the residues involved in catalysis, as well as those involved in binding the carboxylate side chain of the substrate P_1 aspartic acid[27,38] (Fig. 4*e*). Conservation is also high near the Asp–Ser

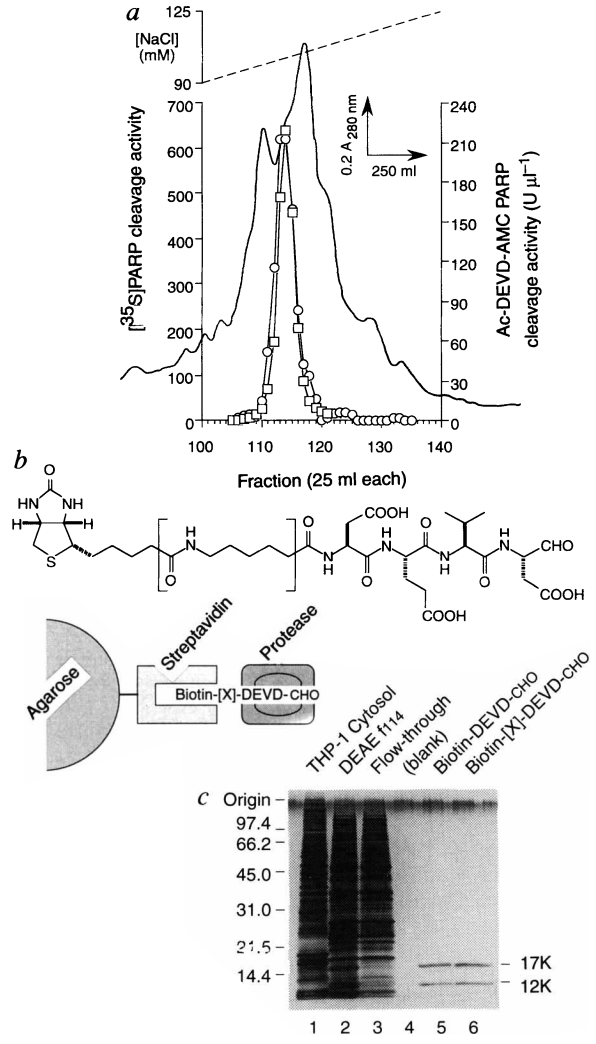

FIG. 3 Purification of the PARP cleavage protease from THP-1 cells. *a*, DEAE anion-exchange chromatography. *b*, Structure of biotinylated tetrapeptide-aldehyde affinity ligands. *c*, SDS–PAGE of THP-1 cell cytosol fraction (lane 1, 9 μg), DEAE peak active fraction (fraction 114) before (lane 2, 6 μg) and after (lane 3, 6 μg) affinity chromatography, eluent from Biotin-DEVD-CHO (lane 5, 0.1 μg) and Biotin-[X]-DEVD-CHO (lane 6, 0.1 μg) affinity columns.

METHODS. *a*, The cytosol fraction from cultured THP-1 cells was isolated, dialysed and concentrated then resolved by anion-exchange chromatography as described previously[46]. Fractions corresponding to approximately 90 to 120 mM NaCl, which immediately followed those containing ICE activity, were pooled, and the pools from 25 chromatography runs were combined (1.6 g protein, from 3.5×10^{12} THP-1 cells) and re-run under identical conditions. PARP cleavage activity was measured using [^{35}S]PARP or the synthetic fluorogenic tetrapeptide-aminomethylcoumarin (Ac-DEVD-AMC) described in Fig. 5. *b*, Biotin-DEVD-CHO and Biotin-[X]-DEVD-CHO differ by the presence of a 0.9 nm spacer arm (square brackets) which is present in Biotin-[X]-DEVD-CHO but absent in Biotin-DEVD-CHO. These ligands were prepared by: synthesis of *t*-Boc-Asp(OBn)-Glu(OBn)-Val-Asp-CHO protected as the benzylated lactol at the aldehyde; removal of the *t*-Boc group; acylation of the free amine with biotin (for Biotin-DEVD-CHO) or biotinamidocaproic acid (for Biotin-[X]-DEVD-CHO) using EDCI and HOBt. *c*, The fraction from DEAE chromatography corresponding to the peak of PARP cleavage activity (fraction 114; 2.5 ml containing 3 mg protein) was incubated with 20 nmol of Biotin-[X]-DEVD-CHO, then passed through a streptavidin-agarose column (1 ml bed volume; binding capacity, 63 nmol biotin ml^{-1}) and washed. The enzyme was eluted by perfusing the column with 2 mM D-biotin. (Biotin-DEVD-CHO yielded comparable results.) Samples were resolved on 14% SDS/polyacrylamide gels, and protein bands were visualized by silver staining.

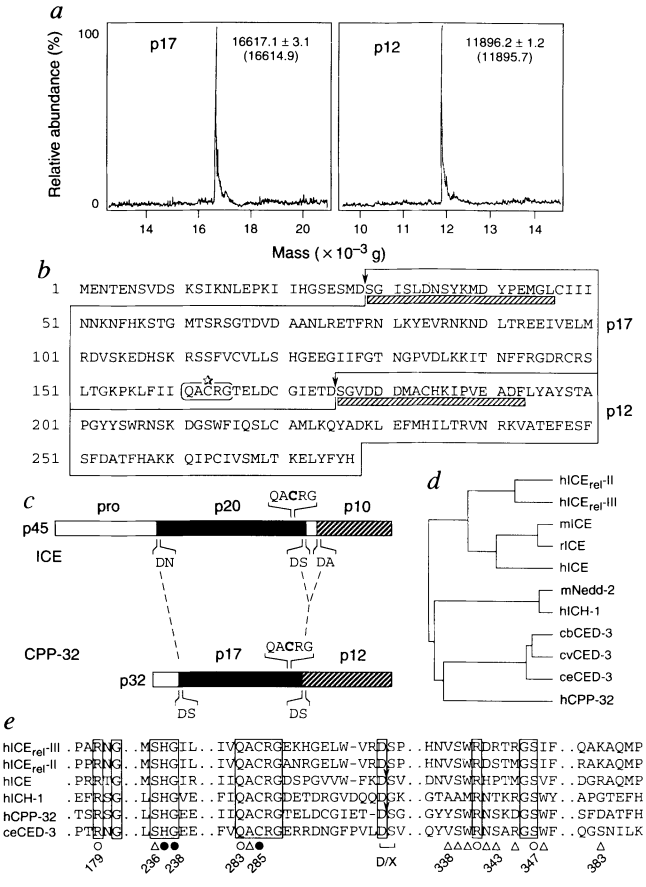

FIG. 4 Structure of PARP cleavage protease; CPP-32. *a*, Electrospray mass spectroscopy analysis of 17K (left) and 12K (right) subunits of the purified PARP cleavage protease. Numbers in brackets indicate the calculated masses of the subunits based on the sequences described in *b*. *b*, Primary structure of CPP-32. The deduced amino-acid sequence from the CPP-32β cDNA clone[26] is shown. Hatched bars indicate the N-terminal sequences determined for the purified enzyme subunits. Arrowheads mark the Asp 28–Ser 29 and Asp 175–Ser 176 cleavage sites which yield the p17 and p12 subunits from the CPP-32 pro-enzyme. *c*, Comparison of ICE and CPP-32 pro-enzyme organization. *d*, Phylogenic relationship of all known members of the ICE/CED-3 family of cysteine protease. *e*, Multiple sequence alignment of all known human ICE/CED-3-like proteases (top 5 sequences) and nematode CED-3 (bottom sequence). Numbering corresponds to the residue position within human ICE. Regions implicated in substrate binding to human ICE, based on the X-ray crystal structure[37,38], are shown: filled circles, catalytic; open circles, binding pocket for carboxylate of P_1 Asp; open triangles, proximity (<0.4 nm) to P_2–P_4 residues. Arrowheads indicate known pro-enzyme cleavage sites for ICE and CPP-32.
METHODS. *a*, Portions of the purified PARP cleavage enzyme described in Fig. 3c were resolved on a narrow-bore C4 reverse-phase HPLC column, and the individual subunits were analysed by capillary liquid chromatography coupled to a triple-sector quadrapole mass spectrometer equipped with an electrospray ion source, essentially as described previously[7]. Tryptic peptides were also generated from the purified subunits and analysed by electrospray mass spectroscopy to further substantiate identification as CPP-32. Peptides and their respective predicted and observed masses were: IPVEADFLYAYSTAPGYYSWR-207, 2470.8, 2470.2; VATEFESFSFDATFHAK-259, 1935.1, 1934.7; LEFMHILTR-238, 1160.4, 1161.0; ELYFYH-277, 872.0, 872.0. *b*, Approximately 100 pmol of the purified PARP cleavage enzyme described in Fig. 3c was resolved on a 14% SDS/polyacrylamide gel and transferred to a polyvinylidenedifluoride membrane for N-terminal sequence determination of the individual p17 and p12 subunits (hatch bars). *d*, *e*, Deduced polypeptide sequences (entire open reading frame) for the indicated cDNA or gene sequences were aligned using the Genetics Computer Group (Madison WI) PILEUP algorithm[47] (gap weight, 3.0; gap-length weight, 0.1) and are presented as a phylogenic dendogram (*d*) and an amino-acid alignment (*e*).

cleavage site at the C terminus of the p20 subunit of ICE (Asp 296–Ser 297) and the p17 of CPP-32 (Asp 175–Ser 176), suggesting that the active forms of the other members of this family are also heterodimers derived from pro-enzymes. Residues that might form the P_2–P_4 binding pockets, however, are not widely conserved, indicating that substrate specificity might be determined by one or more of these amino acids.

Kinetic properties of CPP-32

A continuous fluorometric assay for CPP-32 was developed with the substrate Ac-DEVD-AMC (amino-4-methylcoumarin). The design of this substrate was based on the tetrapeptide-AMC motif that has been used successfully with ICE[7], using the PARP cleavage site P_1–P_4 tetrapeptide (Fig. 5*a* inset). Cleavage of this substrate by CPP-32 showed Michaelis–Menton kinetics with a K_m value of 9.7 ± 1.0 μM (Fig. 5*a*). This assay has facilitated a detailed investigation of the mechanism of inhibition of the enzyme by the tetrapeptide aldehyde Ac-DEVD-CHO.

Peptide aldehydes are potent, reversible inhibitors of cysteine proteases that undergo nucleophilic addition of the catalytic cysteine to form a thiohemiacetal. Although the potency of aldehyde inhibitors was originally attributed to their ability to mimic the transition state in amide bond hydrolysis[39], the recently determined crystal structure of ICE with the tetrapeptide aldehyde Ac-YVAD-CHO clearly shows this inhibitor bound in a non-transition-state conformation, with the oxyanion of the thiohemiacetal being stabilized by the active site histidine[37]. The tetrapeptide aldehyde containing the appropriate recognition sequence for CPP-32, Ac-DEVD-CHO, is a potent, competitive inhibitor of this enzyme. It is slow binding, as shown by the time-dependent approach to equilibrium observed when enzyme was added to reaction mixtures containing inhibitor (50 nM) and $1 \times K_m$ substrate (Fig. 5*b*). The solid line of Fig. 5*b* (filled circles) is theoretical for an association rate constant $k_{on} = 1.3 \times 10^5\ M^{-1}\ s^{-1}$. This rate constant, which is well below theoretical predictions of rates for diffusion-limited reactions (10^8 to $10^{10}\ M^{-1}\ s^{-1}$), is similar to the corresponding rate constant for association of ICE with its tetrapeptide aldehyde inhibitor ($k_{on\ Ac\text{-}YVAD\text{-}CHO} = 3.8 \times 10^5\ M^{-1}\ s^{-1}$). The nearly complete suppression of the activity that was seen at effectively infinite time using 50 nM Ac-DEVD-CHO defines a K_i for inhibition of CPP-32 of <1 nM, making this among the most potent peptide aldehydes known for a cysteine protease.

In contrast to the potent inhibition of CPP-32 observed with the tetrapeptide aldehyde Ac-DEVD-CHO, the ICE inhibitor Ac-YVAD-CHO ($K_{i\,ICE} = 0.76$ nM) is a very weak inhibitor of CPP-32 ($K_{i\,CPP\text{-}32} = 12$ μM), indicating that these enzymes have distinct peptide substrate specificities. This differential in potency can be attributed to the fact that residues implicated in binding the P_4 Tyr of proIL-1β, which is a key determinant for ICE, are not conserved in CPP-32. The crystal structure of active ICE, for example, indicates that the two key amino acids that interact with the P_4 Tyr of proIL-1β are His 342 and Pro 343, which are replaced by Asn and Ser, respectively, in both CPP-32 and CED-3 (Fig. 4*e*). These latter residues in CPP-32 would be better able to form the hydrogen bonds necessary to interact with the carboxylate side chain of the P_4 Asp of PARP. The enzymes also clearly have different macromolecular substrate specificities: purified ICE was unable to cleave PARP, and purified CPP-32 did not cleave proIL-1β at either the FEAD 27–G 28 or DEVD 216–G 217 cleavage sites (a 5,000-fold excess of each enzyme was tested; not shown). The enzymes are also distinguished by their behaviour with the cowpox serpin, CrmA, which shows a 10,000-fold preference for ICE.

The catalytic and inhibitor constants for the PARP cleavage activity in extracts of THP-1 cells, apoptotic osteosarcoma cells,

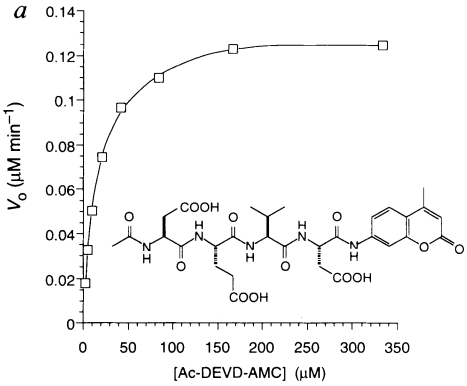

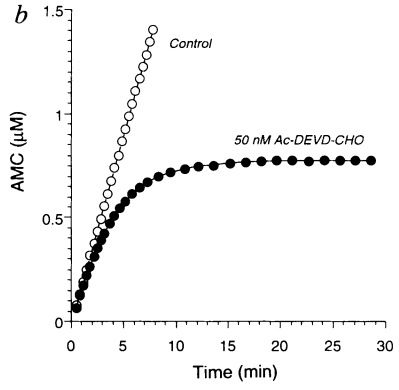

c

Enzyme source	K_m (μM)	k_{on} (M^{-1} s^{-1})	Ac-DEVD-CHO K_i (nM)
THP-1 cells	9.7 ± 1.0	1.3 ± 0.2 x 10^5	< 1
Osteosarcoma cells	10.0 ± 1.1	1.0 ± 0.1 x 10^5	< 1
Chicken S/M extracts	13.6 ± 0.2	1.8 ± 0.1 x 10^5	< 1

FIG. 5 Kinetic parameters for CPP-32 catalysis and inhibition. *a*, Determination of K_m for Ac-DEVD-AMC (structure in insert). *b*, Kinetics of inhibition of CPP-32 by the peptide aldehyde Ac-DEVD-CHO. *c*, Comparison of PARP cleavage activity and inhibition by Ac-DEVD-CHO in THP-1 cell, osteosarcoma cell and chicken S/M extracts.

METHODS. *a*, Ac-DEVD-AMC (inset) was prepared as follows: synthesis of *N*-Ac-Asp(OBn)-Glu(OBn)-Val-CO_2H; coupling with Asp(OBn)-7-AMC; removal of benzyl groups. Reaction mixtures, which contained the indicated concentrations of Ac-DEVD-AMC and 100 U ml^{-1} of the purified PARP-cleavage CPP-32 enzyme (1 U represents 1 pmol AMC liberated per min at 25 °C at saturating substrate concentration), were monitored continuously in a spectrofluorometer at an excitation wavelength of 380 nm and an emission wavelength of 460 nm. Initial velocities and substrate concentrations were fit by nonlinear regression to the Michaelis–Menton equation (solid line). *b*, Reactions contained 1 × K_m Ac-DEVD-AMC (10 μM) and the purified PARP-cleavage CPP-32 enzyme (400 U ml^{-1}). Addition of the tetrapeptide aldehyde (50 nM) to this reaction mixture resulted in a time-dependent loss of enzyme activity (filled circles) whereas the reaction not containing inhibitor was strictly linear (open circles). The association rate constant (k_{on}) was calculated from several progress curves according to equations for slow and tight-binding inhibitors[48]. The complete inhibition of activity observed at infinite time with 50 nM Ac-DEVD-CHO indicates a K_i of less than 1 nM for this inhibitor. *c*, Extracts from THP-1 cells, apoptotic osteosarcoma cells and chicken DU249 cells committed to apoptosis were prepared as described for Fig. 1. The K_m for cleavage of the synthetic fluorogenic tetrapeptide Ac-DEVD-AMC and the k_{on} and K_i values for the tetrapeptide aldehyde inhibitor Ac-DEVD-CHO were determined as described above.

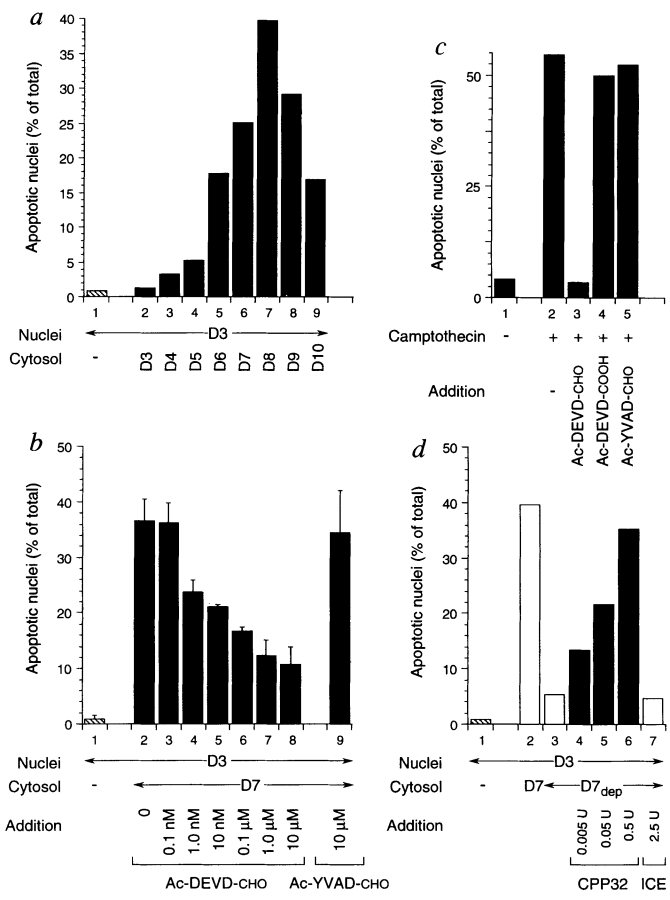

FIG. 6 *In vitro* apoptosis and selective inhibition by Ac-DEVD-CHO or by depletion of CPP-32-mediated PARP cleavage activity. *a*, Cytosols from progressively apoptotic osteosarcoma cells confer apoptotic changes upon healthy nuclei from non-apoptotic cells. *b*, *d*, Attenuation of *in vitro* apoptosis by inhibition or depletion of CPP-32. *c*, Inhibition of camptothecin-induced apoptosis of osteosarcoma cells by Ac-DEVD-CHO.

METHODS. Nuclei were isolated from non-apoptotic (day 3) cells essentially as described before[41], except that the nuclear isolation buffer was 10 mM PIPES/KOH (pH 7.4), 10 mM KCl, 2 mM $MgCl_2$, 1 mM dithiothreitol, 10 μM cytochalasin B, 1 mM phenylmethylsulphonyl fluoride, 10 μg ml^{-1} pepstatin A, 20 μg ml^{-1} leupeptin, 10 μg ml^{-1} aprotinin. *a*, The isolated nuclei from 2 × 10^6 day-3 cells were combined with 25 μl of the cytosol fraction (2.5 × 10^6 cell equivalents) from cells maintained for the indicated times in culture (see Fig. 1) then incubated in 100 μl (final volume) of a mixture containing 10 mM HEPES/KOH (pH 7.0), 50 mM NaCl, 2 mM $MgCl_2$, 0.1 mM $CaCl_2$, 40 mM β-glycerophosphate, 1 mM dithiothreitol, 2 mM ATP, 10 mM creatine phosphate and 50 μg ml^{-1} creatine kinase. After 2 h at 37 °C, nuclear chromatin was stained with 5 μg ml^{-1} Hoechst 33342 and examined by fluorescent microscopy. For each condition, a minimum of 250 nuclei in 5 separate fields were scored. Data are the average of 2 independent experiments. *b*, *In vitro* apoptosis was measured as described in *a* using nuclei from non-apoptotic, day-3 osteosarcoma cells (1–9) combined with the cytosol fraction from apoptotic, day 7 cells (2–9) in the presence of the indicated concentrations of Ac-DEVD-CHO (3–8) or Ac-YVAD-CHO (9). Data are the average of 3 independent experiments ± s.e.m. *c*, Intact day-3 osteosarcoma cell cultures were preincubated for 60 min at 37 °C with vehicle (2) or with 100 μM Ac-DEVD-CHO (3), Ac-DEVD-COOH (4) or Ac-YVAD-CHO (5), then treated with 1 μg ml^{-1} camptothecin (2–5) for an additional 4 h to induce apoptosis. Apoptosis was assessed by fluorescent microscopy as described in *a*. *d*, PARP cleavage activity was depleted from the cytosol fraction of apoptotic, day-7 cells ($D7_{dep}$) by incubating 1 ml of the fraction with 100 nM Biotin-[X]-DEVD-CHO for 20 min then collecting with streptavidin-agarose. *In vitro* apoptosis was measured as described in *a*, using nuclei from non-apoptotic, day-3 osteosarcoma cells (1–7) combined with untreated day-7 cytosol (2) or depleted day-7 cytosol (3–7) supplemented with varying concentrations of purified CPP-32 (4–6) or purified ICE (7).

and apoptotic chicken S/M extracts were virtually identical (Fig. 5*c*), strongly suggesting that the same enzyme (CPP-32) cleaves PARP in all these cell types.

Attenuation of apoptosis

Apoptotic events can be re-constituted *in vitro*. The isolated nuclei from healthy cells undergo the morphological changes that are characteristic of apoptosis (for example, chromatin condensation, fragmentation and margination, as well as internucleosomal DNA cleavage) when they are incubated with the cytosol fraction from apoptotic cells[40,41]. Because the most potent and selective inhibitor of CPP-32-mediated PARP cleavage (Ac-DEVD-CHO) had poor membrane permeability, this system was established with human cells and used to study the effects of CPP-32 inhibition or depletion on apoptosis *in vitro*. Cytosols from non-apoptotic osteosarcoma cells had little effect on nuclear morphology, whereas those from progressively apoptotic cells were capable of inducing apoptosis-like changes in the recipient nuclei (Fig. 6*a*). The degree of apoptotic morphology conferred upon the otherwise healthy nuclei coincided with the degree of apoptosis occurring in the cells from which the cytosols were extracted (see Fig. 1*c*) as well as the level of PARP cleavage activity (see Fig. 1*d*).

If the PARP-cleaving CPP-32 cysteine protease is important for apoptosis then inhibition or depletion of its activity should prevent these nuclear changes from occurring. Morphological changes that occurred when the cytosol fraction from apoptotic osteosarcoma cells was incubated with healthy nuclei from non-apoptotic cells could be attenuated by the tetrapeptide aldehyde inhibitor of CPP-32-mediated PARP cleavage, Ac-DEVD-CHO (IC_{50} = 10 to 100 nM), but not with the ICE inhibitor, Ac-YVAD-CHO (Fig. 6*b*). The camptothecin-stimulated apoptotic death of intact osteosarcoma cells was also prevented by Ac-DEVD-CHO (albeit at high concentrations only (100 μM)), whereas neither the inactive carboxylic acid (Ac-DEVD-COOH) nor the ICE inhibitor (Ac-YVAD-CHO) had any effect (Fig. 6*c*). Furthermore, if CPP-32 were depleted from the cytosol fraction of apoptotic osteosarcoma cells using the biotinylated affinity ligand, these PARP cleavage-deficient extracts were largely incapable of conferring apoptotic changes to healthy recipient nuclei (Fig. 6*d*). The pro-apoptotic capabilities of depleted extracts were restored when they were supplemented with purified CPP-32, but not when they were supplemented with purified ICE. In the absence of a cytosolic fraction, CPP-32 alone did not provoke apoptotic changes to healthy nuclei (not shown), demonstrating that CPP-32 is necessary but not sufficient for apoptosis. Together, these experiments suggest that CPP-32 initiates key events in apoptosis and that inhibition or depletion of its activity prevents apoptosis from occurring.

Conclusions

In the nematode *C. elegans*, deletion or mutation of a single gene, *ced-3*, abolishes apoptotic death[5]. When sequenced, *ced-3* was found to be homologous to the gene for mammalian interleukin-1β-converting enzyme (ICE)[6], which encodes a protease whose only known function is the cleavage of the inactive 31K proIL-1β cytokine precursor to the active 17K form. How the apoptotic role of an ICE-like protease in mammalian cells can be accounted for, given the commitment of ICE to IL-1β formation, and the finding that apoptosis occurs normally in ICE-deficient mice[29,30], has become more obvious with the discovery of four other mammalian ICE/CED-3-like proteases (ICE_{rel}-II, ICE_{rel}-III, Nedd-2/ICH-1 and CPP-32)[24–27] and the observation that PARP, an enzyme involved in the coordination of genome structure and integrity in stressed cells, is functionally inactivated by a protease resembling ICE (prICE) at the onset of apoptosis[20]. We have demonstrated that prICE is in fact CPP-32, and that CPP-32 is the specific ICE/CED-3-like cysteine protease that cleaves PARP in mammalian cells. The name apopain is proposed for the active form of this enzyme to replace prICE and CPP-32. The central role played by CPP-32/apopain in mammalian cell death is further substantiated by potent and selective inhibitors that prevent apoptosis from occurring *in vitro* and *in vivo*. These findings, together with the sequence relationship between CPP-32 and CED-3, suggests that CPP-32 may be the human equivalent of CED-3. The pharmacological modulation of CPP-32/apopain activity may therefore be an appropriate point for therapeutic intervention in pathological conditions where inappropriate apoptosis is prominent. □

Received 3 March; accepted 24 May 1995.

1. Kerr, J. F., Wyllie, A. H. & Currie, A. R. *Br. J. Cancer* **26,** 239–257 (1972).
2. Martin, S. J., Green, D. R. & Cotter, T. G. *Trends biochem. Sci.* **19,** 26–30 (1994).
3. Barr, P. J. & Tomei, L. D. *Biotechnology* **12,** 487–493 (1994).
4. Carson, D. A. & Ribeiro, J. M. *Lancet* **341,** 1251–1254 (1994).
5. Ellis, R. E., Yuan, J. & Horvitz, H. R. *A. Rev. Cell Biol.* **7,** 663–698 (1991).
6. Yuan, J., Shaham, S., Ledoux, S., Ellis, J. M. & Horvitz, J. R. *Cell* **75,** 641–652 (1993).
7. Thornberry, N. A. *et al. Nature* **356,** 768–774 (1992).
8. Cerretti, D. P. *et al. Science* **256,** 97–100 (1992).
9. Miura, M., Zhu, H., Rotello, R., Hartwieg, E. A. & Yuan, J. *Cell* **78,** 653–660 (1993).
10. Gagliardini, V. *et al. Science* **263,** 826–828 (1994).
11. Juarez-Salinas, H., Sims, J. L. & Jacobson, M. K. *Nature* **282,** 740–741 (1979).
12. Berger, N. A., Sikorski, G. W., Petzold, S. J. & Kurohara, K. K. *Biochemistry* **19,** 289–293 (1980).
13. Satoh, M. S. & Lindahl, T. *Nature* **356,** 356–358 (1992).
14. Ding, R., Pommier, Y., Kang, V. H. & Smulson, M. *J. biol. Chem.* **267,** 12804–12812 (1992).
15. Smulson, M., Istock, N., Ding, R. & Cherney, B. *Biochemistry* **33,** 6186–6194 (1994).
16. Ding, R. & Smulson, M. *Cancer Res.* **54,** 4627–4634 (1994).
17. Bürkle, A., Grube, K. & Küpper, J.-H. *Expl clin. Immunogenet.* **9,** 230–240 (1992).
18. Wang, Z. Q. *et al. Genes Dev.* **9,** 509–520 (1995).
19. Kaufmann, S. H., Desnoyers, S., Ottaviano, Y., Davidson, N. E. & Poirier, G. G. *Cancer Res.* **53,** 3976–3985 (1993).
20. Lazebnik, Y. A., Kaufmann, S. H., Desnoyers, S., Poirier, G. G. & Earnshaw, W. C. *Nature* **371,** 346–347 (1994).
21. Yoshihara, K., Tanigawa, Y. & Koide, S. S. *Biochem. biophys. Res. Commun.* **59,** 658–665 (1974).
22. Yoshihara, K., Tanigawa, Y., Burzio, L. & Koide, S. S. *Proc. natn. Acad. Sci. U.S.A.* **72,** 289–293 (1975).
23. Tanaka, Y., Yoshihara, K., Itaya, A., Kamiya, T. & Koide, S. S. *J. biol. Chem.* **259,** 6579–6585 (1984).
24. Kumar, S., Kinoshita, M., Noda, M., Copeland, N. G. & Jenkins, N. A. *Genes Dev.* **8,** 1613–1626 (1994).
25. Wang, L., Miura, M., Bergeron, L., Zhu, J. & Yuan, J. *Cell* **78,** 739–750 (1994).
26. Fernandes-Alnemri, T., Litwack, G. & Alnemri, E. S. *J. biol. Chem.* **269,** 30761–30764 (1994).
27. Munday, N. A. *et al. J. biol. Chem.* **270,** 15870–15876 (1995).
28. Williams, M. S. & HenKart, P. A. *J. Immun.* **153,** 4247–4255 (1994).
29. Heusel, J. W., Wesselschmidt, R. L., Shresta, S., Russell, J. H. & Ley, T. J. *Cell* **76,** 977–987 (1994).
30. Li, P. *et al. Cell* **80,** 401–411 (1995).
31. Kuida, K. *et al. Science* **267,** 2000–2003 (1995).
32. Enari, M., Hug, H. & Nagata, S. *Nature* **375,** 78–81 (1995).
33. Los, M. *et al. Nature* **375,** 81–83 (1995).
34. Ayala, J. M. *et al. J. Immun.* **153,** 2592–2599 (1994).
35. Ray, C. A. *et al. Cell* **69,** 597–604 (1992).
36. Howard, A. D. *et al. J. Immun.* **154,** 2321–2332 (1995).
37. Wilson, K. P. *et al. Nature* **370,** 270–275 (1994).
38. Walker, N. P. C. *et al. Cell* **78,** 343–352 (1994).
39. Westerik, J. O. & Wolfenden, R. *J. biol. Chem.* **247,** 8195–8197 (1972).
40. Solary, E., Bertrand, R., Kohn, K. W. & Pommier, Y. *Blood* **81,** 1359–1368 (1993).
41. Lazebnik, Y. A., Cole, S., Cooke, C. A., Nelson, W. G. & Earnshaw, W. C. *J. Cell Biol.* **123,** 7–22 (1993).
42. deMurcia, G., Ménissier-deMurcia, J. & Schreiber, V. *BioEssays* **13,** 455–462 (1991).
43. Langlois, A. J., Lapis, K., Ishizaki, R., Beard, J. W. & Bolognesi, D. P. *Cancer Res.* **34,** 1457–1464 (1974).
44. Cherney, B. W. *et al. Proc. natn. Acad. Sci. U.S.A.* **84,** 8370–8374 (1987).
45. Chapman, K. T. *Bioorg. Med. Chem. Lett.* **2,** 613–618 (1992).
46. Miller, D. K. *et al. J. biol. Chem.* **268,** 18062–18069 (1993).
47. Devereux, J., Haeberli, P. & Smithies, O. *Nucleic Acids Res.* **12,** 387–395 (1984).
48. Morrison, J. F. *Trends biochem. Sci.* **7,** 102–105 (1982).

ACKNOWLEDGEMENTS. We thank L. Quan and G. Salvesen for providing us with purified CrmA.